Photoreflectance study on residual strain in heteroepitaxial gallium arsenide on silicon

T. Kanata, H. Suzawa, M. Matsunaga, H. Takakura, and Y. Hamakawa
Department of Electrical Engineering, Faculty of Engineering Science, Osaka University, Toyonaka-shi, Osaka 560, Japan

H. Kato
Department of Physics, Faculty of Science, Kwansei Gakuin University, Uegahara, Nishinomiya 662, Japan

T. Nishino
Department of Electrical Engineering, Faculty of Engineering, Kobe University, Rokkodai-cho, Nada-ku, Kobe 657, Japan
(Received 19 June 1989)

The effect of residual strain on photoreflectance (PR) signals near the heteroepitaxial interface in gallium arsenide (GaAs) grown directly on a silicon substrate has been systematically investigated. With use of data on the stress-induced splitting and the shift of the E_0 (Γ_{8v}-Γ_{6c}) fundamental transition, the distribution of residual strain in the vicinity of the heteroepitaxial interface in the GaAs layer has been evaluated. It has been found that compressive strain caused by the lattice mismatch between the materials is not completely compensated and is about 0.4% near the heterointerface in the GaAs layer grown at relatively low growth temperature. This compressive strain gradually relaxes with increasing thickness and then transforms to tensile strain around thicknesses greater than 2 μm. The residual tensile strain at the surface of a 3.6-μm-thick GaAs layer is about 0.2%. In the thickness range from 0.5 to 2 μm, the observed PR spectra demonstrate the presence of two regions with different strain in the epitaxial layer. For thicknesses less than 0.5 μm, crystal quality is degraded by defects associated with misfit compensation during the initial stage of growth.

I. INTRODUCTION

Recently, heteroepitaxial-growth technology of gallium arsenide (GaAs) on a silicon (Si) substrate has attracted much attention because of the promise of hybridization of GaAs integrated circuits (IC's) with Si IC's and high-efficiency solar cells. Recently laser[1,2] and field-effect transistors[3,4] (FET's) have been developed, and high-efficiency (more than 18%) solar cells[5] have been fabricated with heteroepitaxially grown GaAs on a Si substrate. The key issue of success in this technology is the elucidation of a mechanism for the accommodation of a large residual strain in the GaAs layer. Residual strain is introduced in GaAs films as a result of the different lattice constant and thermal-expansion coefficient of the constituent materials.[6-11] The structural, electrical, and optical properties of this heterostructure depend strongly on such internal strain. The lattice mismatch between two materials is 4.1% at room temperature (25 °C) and 4.2% at the growth temperature (570 °C). This lattice mismatch induces biaxial compressive strain in the GaAs film. It is generally believed that this strain is completely relaxed by the formation of misfit dislocations during the growth because of the very thin critical layer thickness (less than several angstroms). On the other hand, the difference of the thermal-expansion coefficient between the constituent materials is large. This large difference induces bimetal-type tensile stress in the GaAs film, when the substrate temperature is cooled down from the growth temperature to room temperature.

Many reports on thermally induced biaxial strain in this particular material combination have been published,[6-11] showing that the observed strain depends strongly on the thickness and growth temperature. In particular, compressive strain has been observed in the GaAs epitaxial films grown at relatively low temperature (< 420 °C).[8] These experimental results suggest that compressive strain caused by lattice mismatch is not completely compensated at the initial growth stage. This experiment has been performed to examine the accommodation process of this strain in the epitaxial GaAs film grown by molecular-beam epitaxy (MBE) on a Si substrate at a relatively low growth temperature (570 °C).

The residual stress and strain have been studied by photoreflectance (PR). A modulation spectroscopy, PR is a reflectance modulation produced by a secondary light beam,[12-14] which is a "contactless" form of electroreflectance (ER). It is possible to easily observe the signals due to the fundamental-band edge even at room temperature by this reflectance modulation. With use of this PR method, characterization of semiconductors and semiconductor microstructures such as superlattices and heterostructures has been performed.[15-20] This electromodulation technique was especially powerful for the investigation of stress effects in semiconducting materials, such as the determination of deformation potentials.[21-23]

In this work, thickness dependences of the residual strain have been carefully studied by PR measurements. The PR spectra have been analyzed to elucidate a possi-

ble mechanism for the accommodation process of the strain in the vicinity of the heteroepitaxial interface in the GaAs layer grown on a Si substrate.

II. EXPERIMENTAL DETAILS

A. Growth of GaAs on a Si substrate

GaAs single crystals were grown on a Si substrate by MBE. The GaAs growth was monitored by reflection high-energy electron diffraction (RHEED) during the growth, and single-monolayer growth was confirmed by oscillations in the RHEED pattern.[24] Si substrates are tilted at 4° away from the [001] orientation toward the [110] direction, and the thickness was 300 or 500 μm. In order to reduce contamination by carbon and heavy metals, the Si substrate with a thin oxide film was loaded in the growth chamber of the MBE system, and the oxide film was removed thermally above 750 °C for 10 min just before the growth.[25] The cleaned Si substrate showed the single-domain 2×1 reconstructed surface. After the oxide dissociation, the substrate temperature was lowered to 300 °C, and a nucleation layer of 20-nm-thick GaAs was grown at a slow growth rate of 6 monolayers/min at 300 °C. A spotty RHEED pattern was observed in this stage. This shows the island growth with small grains. The growth temperature was then raised to 570 °C under As_4 flux. At this temperature, solid-phase epitaxy (SPE) was performed for 5 min. The spotty pattern of RHEED changed gradually to an arrowheadlike shape, and finally a clear streak pattern appeared which is associated with the 2×4 reconstructed surface. After this SPE, the GaAs layer was grown at a growth rate of 1 monolayer/s at 570 °C. The oscillation in the RHEED pattern at this stage is shown in Fig. 1; the peak-to-peak time interval corresponds to a single monolayer in the growth process. The 2×4 reconstructed surface was observed during the growth.

Two types of samples were prepared. One is 3.6-μm-thick GaAs doped with 1×10^{17} cm^{-3} Si grown on the 300-μm-thick substrate and the other is undoped 1-μm-thick GaAs grown on the 500-μm-thick substrate. The etch-pit density (EPD) of these two GaAs crystals was 1.3×10^{7} cm^{-3} for the 3.6-μm-thick GaAs and 4.8×10^{7} cm^{-3} for the 1-μm-thick GaAs. To investigate the thickness dependence on PR spectra, the GaAs film was etched by a mixing solution of $[H_2SO_4]$:$[H_2O_2]$:$[H_2O]$ = 6:1:1 at 4 °C with the rate of 0.2 μm for one step. The etching rate was 16 nm/s.

B. PR measurement

PR, which is a contactless form of electromodulation spectroscopy, is a useful tool to study the interband transitions in a strained semiconductor, because even at room temperature, one can observe sharp and derivativelike spectra of all allowed transitions. A schematic representation of the experimental arrangement for PR measurements is shown in Fig. 2. The reflectance modulation was achieved by photoexcited electron-hole pair generation due to a secondary photon source. A 2-mW He-Ne laser (operating at a wavelength of 632.8 nm) chopped at 80 Hz was used for this purpose. The typical power density on a sample was about 1 mW/cm^2. The probe light from a tungsten lamp passed through the monochromator was irradiated on the surface of GaAs film at near-normal reflection alignment with a reflection angle smaller than 30°. The reflected light intensity was detected by a photomultiplier (PM). The PR signal ($\Delta R/R$) was obtained by the phase-sensitive detection of the ac component (corresponding to a change in reflectivity, ΔR) through a lock-in amplifier under the condition that the dc component of the photomultiplier (corresponding to the reflectivity R) was kept constant by changing the high voltage through an electronic feedback circuit, i.e., controlling the sensitivity of PM. All the PR measurements were performed at room temperature (25 °C).

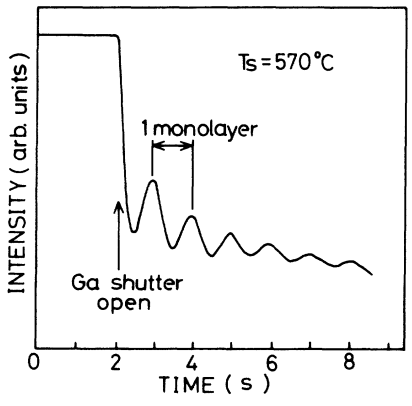

FIG. 1. Oscillation of the specular beam with the [110] azimuth in the RHEED pattern from the GaAs(001)-2×4 reconstructed surface. The period exactly corresponds to the growth of a single monolayer.

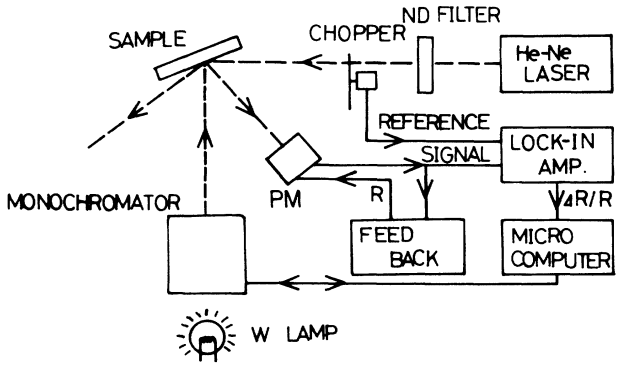

FIG. 2. Block diagram of photoreflectance measurement system.

III. THEORETICAL BACKGROUND

A. Transitions at $\mathbf{k}=0$ under stress

In the GaAs/Si system, stress (strain) originates mainly from a large thermal-expansion mismatch between the constituent materials, if the compressive stress caused by large lattice mismatch (4.2% at the growth temperature of 570 °C) is assumed to be relaxed by the formation of misfit dislocations during the growth of GaAs on a Si substrate. The stress caused by thermal-expansion mismatch was discussed in detail by Feng *et al.*[26] Assuming that the Young's modulus of GaAs and its difference between room and growth temperatures are almost the same as those of Si, the stress at the surface of GaAs epitaxial form is written

$$\sigma=\frac{E\,\Delta T}{d^2}d_{\mathrm{Si}}(2d_{\mathrm{GaAs}}-d_{\mathrm{Si}})(\alpha_{\mathrm{GaAs}}-\alpha_{\mathrm{Si}})\ , \tag{1}$$

where α_{GaAs} and α_{Si} are the thermal-expansion coefficients, and the thickness d is given by the relation $d=d_{\mathrm{GaAs}}+d_{\mathrm{Si}}$. Figure 3 shows this stress and strain calculated as a function of the thicknesses of epitaxial film and substrate.

For a zinc-blende–type material such as GaAs, the valence-band edge at $\mathbf{k}=\mathbf{0}$ is a sixfold-degenerate multiplet with orbital symmetry Γ_{15}, which consists of a fourfold $P_{3/2}$ multiplet [$(J=\frac{3}{2}, m_j=\pm\frac{3}{2},\pm\frac{1}{2})$ in spherical notation] and a twofold $P_{1/2}$ multiplet, $(J=\frac{1}{2}, m_j=\pm\frac{1}{2})$. The application of biaxial stress splits the $P_{3/2}$ multiplet, because of the reduced symmetry.[22,23] The hydrostatic-pressure component of the strain results in a shift of centers of gravity of the $P_{3/2}$ and $P_{1/2}$ multiplets relative to the conduction band.[22,23] In this experiment, we examined the $P_{3/2}$ multiplet. The bands are labeled HH($J=\frac{3}{2}$, $m_j=\pm\frac{1}{2}$) and LH($J=\frac{3}{2}$, $m_j=\pm\frac{3}{2}$) in this paper. It has been shown that the orbital-strain Hamiltonian H_s for a given band at $\mathbf{k}=\mathbf{0}$ can be written as[22]

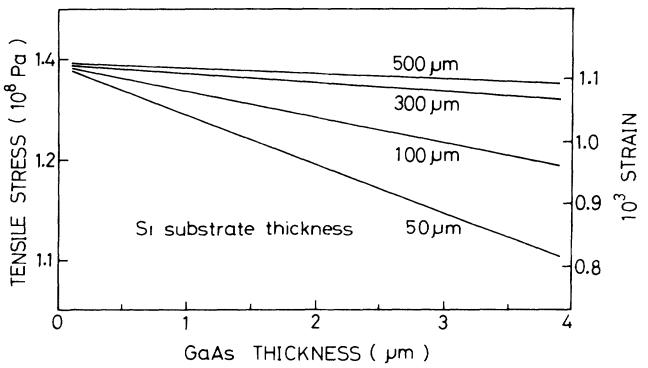

FIG. 3. Theoretical calculation of tensile stress caused by thermal-expansion mismatch in GaAs on a Si substrate, assuming no compressive stress at the growth temperature.

$$H_s=-a(e_{xx}+e_{yy}+e_{zz})-3b[(L_x^2-\mathbf{L}^2/3)e_{xx}+\mathrm{c.p.}]-\frac{6d}{\sqrt{3}}(\tfrac{1}{2}\{L_x,L_y\}e_{xy}+\mathrm{c.p.})\ , \tag{2}$$

where e_{ij} is the component of strain tensor, $\mathbf{L}$ is the angular-momentum operator, c.p. denotes cyclic permutations with respect to indices x, y, and z, and the quantities in the curly brackets indicate the anticommutator $\{L_x,L_y\}\equiv L_xL_y+L_yL_x$. The quantity a is the hydrostatic-deformation potential, and b and d are the shear-deformation potentials appropriate to strain of tetragonal and rhombohedral symmetries, respectively. For biaxial stress, that is, $\sigma_{xx}=\sigma_{yy}=\sigma$ and $\sigma_{zz}=0$, and all mixed terms xy, xz, and yz are zero, the strain components are

$$e_{xx}=e_{yy}=(S_{11}+S_{12})\sigma\ , \tag{3a}$$

$$e_{zz}=2S_{12}\sigma\ , \tag{3b}$$

$$e_{xy}=e_{xy}=e_{yz}=0\ , \tag{3c}$$

where σ is stress which is positive for compressive stress. S_{11} and S_{12} are elastic compliance constants. From Eqs. (2) and (3a)–(3c), H_s is rewritten by

$$H_s=-2a(S_{11}+2S_{12})\sigma+3b(S_{11}-S_{12})\sigma(L_z^2-\mathbf{L}^2/3) \tag{4}$$

and becomes

$$H_s=-\delta E_H^v-\tfrac{3}{2}\delta E_s(L_z^2-\mathbf{L}^2/3)\ , \tag{5}$$

where $\delta E_H^v=2a(S_{11}+2S_{12})\sigma$, which indicates the shift of center of gravity of the $P_{3/2}$ multiplet, due to the hydrostatic component of strain, and $\delta E_S=-2b(S_{11}-S_{12})\sigma$, which indicates the linear splitting of this multiplet. On the other hand, the conduction band does not split under the application of stress, but shifts by the hydrostatic component of strain. This energy shift for the conduction band is denoted by δE_C. Therefore, the change in energy for the lowest direct gap is given by

$$\delta E_{C\text{-LH}}=\delta E_H+\tfrac{1}{2}\delta E_S\ , \tag{6a}$$

$$\delta E_{C\text{-HH}}=\delta E_H+\tfrac{1}{2}\delta E_S\ , \tag{6b}$$

where $\delta E_H=\delta E_C+\delta E_h^v$. In Eq. (6b), the higher-order terms were neglected because of relatively small residual strain (Fig. 3).

B. PR spectra

Reflectance modulation in PR is caused by the modulation of built-in electric field in the surface potential barrier due to photoexcited barriers. The built-in electric field produced by surface states is described by Poisson's equation. The electric field $\Theta(z)$ as a function of the distance z from the surface is written by

$$\Theta(z)=eN_D(W-z)/(\epsilon_0\epsilon_r)\ , \tag{7}$$

where e is the electron charge, ϵ_0 the dielectric constant of vacuum, ϵ_r the relative dielectric constant, and N_D the

donor concentration of a sample. W is the depletion-region width and is given by

$$W=[2\epsilon_r\epsilon_0\phi/(eN_D)]^{1/2} , \quad (8)$$

where ϕ is the built-in potential. Equations (7) and (8) indicate that the electric field depends on N_D and ϕ.

In the low-field regime, the $\Delta R/R$ spectra are expressed by a derivative line shape of the dielectric function,[18,27,28]

$$\Delta R/R=\mathrm{Re}\left[\sum_{j=1}^{p} C_j e^{i\theta_j}(E-E_{g,j}+i\Gamma_j)^{-m_j}\right] , \quad (9)$$

where p is the number of interband transitions included, and C_j, θ_j, $E_{g,j}$, Γ_j, and m_j are the amplitude, phase factor, energy, broadening parameter, and a parameter that depends on critical point type and order of derivative of the jth feature, respectively. In the surface barrier of a semiconductor, the modulating light power P, the modulated surface voltage V by the modulating light, and the average field $\bar{\Theta}$ have the following relation:

$$\ln(P)\propto V\propto \bar{\Theta}^2 , \quad (10)$$

where $\Delta R/R$ is proportional to $\bar{\Theta}^2$ in this field range.[28] Therefore, $\Delta R/R$ is proportional to $\ln(P)$ in low-field regime.

In the intermediate-field regime,[28] we must treat carefully the modulating field which consists of an ac electric field Θ_{ac} and a built-in dc electric field Θ_{dc} because the period of the observed Franz-Keldysh (FK) oscillations and the envelope function are related to Θ_{dc} and Θ_{ac}/Θ_{dc}, respectively.[14] In PR measurements, the built-in electric field Θ_{dc} is larger than Θ_{ac}. Therefore, the theory based on the modulation from the flat band[29] cannot be applied directly to an analysis of the PR spectrum. Recently, Bhattacharya *et al.*[14] treated electromodulation under the conditions of a large Θ_{dc} ($>\Theta_{ac}$). They give the perturbed dielectric function $\delta\epsilon(E,\Theta^s_{dc},\Theta^s_{ac})$ by

$$\delta\epsilon(E,\Theta^s_{dc},\Theta^s_{ac})\propto\frac{1}{E^2}(\Theta^s_{dc})^{1/3}\times\Theta^s_{ac}[\tilde{G}(\eta^s_{dc},\xi)+i\tilde{F}(\eta^s_{dc},\xi)] , \quad (11)$$

where Θ^s_{dc} and Θ^s_{ac} are the surface dc and ac electric fields, respectively. The functions $\tilde{F}(\eta^s_{dc},\xi)$ and $\tilde{G}(\eta^s_{dc},\xi)$ are the newly defined functions in Ref. 14. Here,

$$\eta^s_{dc}=(E_g-E)/\hbar\theta^s_{dc} , \quad (12a)$$

$$(\hbar\theta^s_{dc})^3=(e\hbar\Theta^s_{dc})^2/2\mu , \quad (12b)$$

$$\xi=\Theta^s_{ac}/\Theta^s_{dc} , \quad (12c)$$

and $\hbar$ is Planck's constant and μ the reduced interband mass.

Since the Seraphin coefficients α and β are $\alpha\gg\beta$ around the band edge E_g^0 (1.428 eV) of unstrained GaAs at 300 K, $\Delta R/R$ is determined by the real part of Eq. (11). The observed PR signal is the summation of the contribution of the transitions from the light and heavy holes to the s-like conduction band. Therefore, $\Delta R/R$ is given by

$$\Delta R/R=(\Delta R/R)_l+(\Delta R/R)_h , \quad (13)$$

where $(\Delta R/R)_l$ and $(\Delta R/R)_h$ are the PR signals related to light and heavy holes, respectively.

IV. EXPERIMENTAL RESULTS AND DISCUSSIONS

Figure 4 shows the thickness dependence of PR spectra of 3.6-μm-thick GaAs ($N_D=1\times10^{17}$ cm^{-3}). In these PR spectra, two major features are observed: (i) The PR spectrum drastically changes around the thickness of 2.0 μm, and (ii) FK oscillation is observed at more than 1.5 eV in each spectrum. The modulation-light-power dependence of the PR signal was carefully investigated in the range 0.01–10.0 mW/cm^2. Although the clear change of the amplitude of PR spectra was observed, there is no change in the line shape of the spectra. The dependence of PR amplitude on $\ln(P)$ does not show the low-field properties as demonstrated by Eq. (10). This result and FK oscillation in Fig. 4 indicates that the PR line shape of this heavily doped sample is explained by the modulation in the intermediate-field regime. The identical line shape in the range 0.01–10.0 mW/cm^2 does not always mean that the PR spectra are in the low-field regime. According to the recent theoretical and experimental investigations by Bhattacharya *et al.*,[14] PR line shapes measured at the various modulating light intensities are identical, when the modulating field is very small

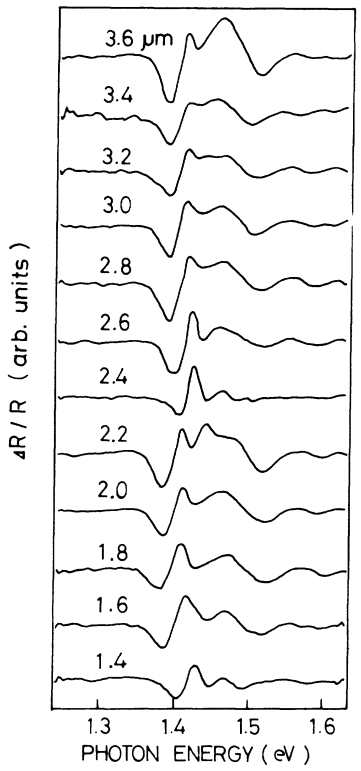

FIG. 4. Thickness dependence of PR spectra of 3.6-μm-thick GaAs ($N_D=1\times10^{17}$ cm^{-3}).

compared to the built-in field. In PR measurements, the built-in electric field is larger than the modulating field.[14] Therefore, it can be considered that the spectra in Fig. 4 are in the intermediate-field modulation. If the observed PR spectra are the superposition of the relatively sharp exciton spectrum and the interband transitions, the amplitude, phase, and broadening of the spectral line shape associated with the exciton are extremely sensitive to the magnitude of the modulating and dc bias voltage, i.e., the modulating light power in the PR measurement.[14,23,30] Since the line shape in the range of the modulating light intensity from 0.01 to 10.0 mW/cm^2 is identical, the prominent feature in PR spectra in Fig. 4 is due to the nonexcitonic interband transitions. The heteroepitaxial films have a large dislocation density greater than 10^7 cm^{-3}. This dislocation almost quenches the exciton in GaAs film at room temperature. Therefore, it is considered that the signal from the quenching of the exciton by the applied field could not be observed in PR measurements.

The PR spectral profile in the intermediate-field regime can be simulated theoretically from Eqs. (11)–(13). Figure 5 shows a comparison between the calculated and experimental PR spectra at 2.8 μm. The power density of the modulating light was 10.0 mW/cm^2. In this calculation, spectral broadening was not considered, and the amplitudes of spectra originated from light and heavy holes were taken as fitting parameters. The band-edge energies, the period of FK oscillations, and its damping profile give the information about the stress effect and the built-in electric field. We have obtained the following values from this analysis: $\delta E_{C\text{-}LH}=-8$ meV, $\delta E_{C\text{-}HH}=-38$ meV, $\Theta^s_{dc}=1.0\times10^5$ V/cm ($\phi=0.33$ V), and $\xi=0.21$. It can be seen that the calculated band-edge energy and oscillation period agree well with those of the experimental PR spectrum. According to Eqs. (7) and (8), the built-in surface electric field Θ^s_{dc} and the space-charge width W of this sample are 1.4×10^5 V/cm and 103 nm, respectively. In this calculation, we assumed $\phi=0.7$ V, which corresponds Fermi-level pinning below the conduction band.[31] It is noted that the calculated Θ^s_{dc} is smaller than the value expected by Fermi-level pinning. The evaluated ξ indicates that the modulating field at the maximum modulating-light intensity of 10.0 mW/cm^2 is about 1 order of magnitude smaller than the built-in field. The identical line shape observed in the range of the modulating light intensity from 0.01 to 10.0 mW/cm^2 can be explained by this small value of ξ.[14] Applying the similar analytical process to the other spectra, the band edges were obtained as a function of the thickness of GaAs film. The results will be discussed later.

For 1-μm-thick GaAs (undoped), the same PR measurement was performed. The results are shown in Fig. 6. In this case, FK oscillations were not observed in a higher-energy region. Figure 7 shows the modulating-light-power dependence of the PR amplitude of $\Delta R/R$. It can be seen that $\Delta R/R$ increases in proportion to $\ln(P)$. According to Eq. (10), these PR line shapes are explained by the low-field ER theory expressed by Eq. (9). Furthermore, it was found that the prominent spectral features in Fig. 6 are due to the nonexcitonic interband transitions, because the change of the spectral features was not observed by varying the modulating-light intensity. In the photoluminescence (PL) experiments[6,10] at low temperature for GaAs/Si, the spectra originating from the two different strain regions were observed in the sample with some cracks in the GaAs film, and the actual splitting of the valence-band degeneracy in each region was observed by PL excitation measurement, that is, four valence bands exist in the sampling region. In the sample having only small cracks, the PL spectrum ascribed to only one kind of strain region in the GaAs film is ob-

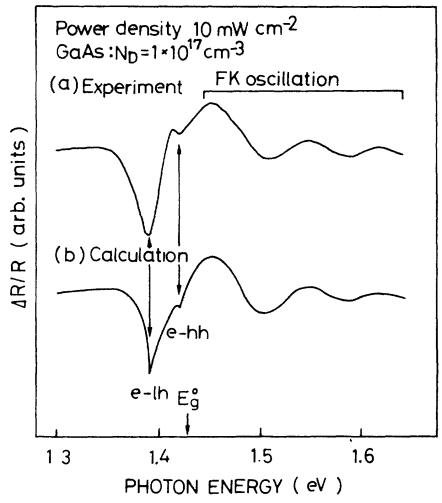

FIG. 5. (a) Experimental PR spectrum of GaAs ($N_D=1\times10^{17}$ cm^{-3}) at 2.8 μm, and (b) theoretically calculated PR spectrum.

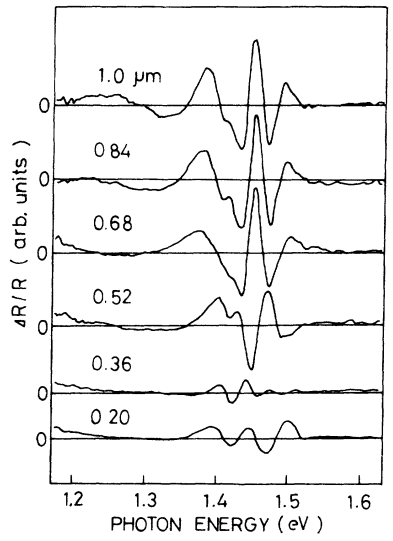

FIG. 6. Thickness dependence of PR spectra of 1-μm-thick GaAs (undoped).

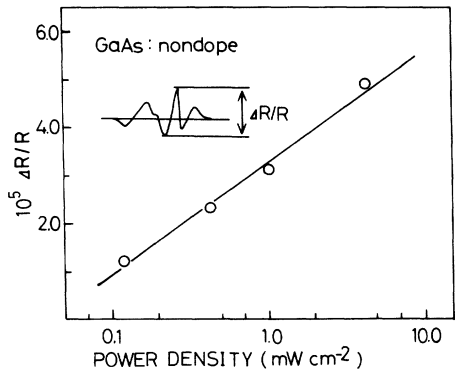

FIG. 7. Pumping-light-power dependence of the amplitude of $\Delta R/R$.

served.[10] Since it was checked by an electron-beam-induced current (EBIC) image that the samples measured in this experiment clearly have some cracks in the GaAs films,[32] the former case is possible; that is, two different strain regions cause the splitting of the valence-band splitting in each region in our samples. Therefore, we try to explain the PR spectra by a superposition of four line-shape functions described by Eq. (9). In this calculation, $m_j = \frac{5}{2}$ is appropriate for the observed PR spectra due to the nonexcitonic nature of these features. Figure 8(a) shows a typical result of the least-squares fit of Eq. (9) for $m_j = \frac{5}{2}$ to the experimental PR spectra. The solid and dashed lines are the measured and calculated PR spectra, respectively. The calculated line shape is the summation of four different PR spectra plotted in Fig. 8(c). Figure 8(b) shows the difference between the experimental and calculated PR spectra, and indicates a ground agreement between them. Since the accuracy in the evaluation of the band gaps $E_{g,j}$ for each critical point was within 5 mV, this calculation can be considered to be unique. In the thickness dependence of the PR spectrum shown in Fig. 6, each peak position gradually changes with decreasing the thickness. For thicknesses less than 0.5 μm, however, the PR signal becomes extremely weak and it is very difficult to determine $E_{g,j}$ precisely from the fitting of the spectra. This result indicates that the crystal quality is degraded by defects associated with the misfit compensation during the initial stage of growth.

The $E_{g,j}$ evaluated from PR spectra in Figs. 4 and 6 are plotted as a function of the film thickness in Fig. 9. The data of Figs. 4 and 6 are expressed by the open and solid circles, respectively. The dash-dotted line shows the position of E_g^0. According to Eqs. (6a) and (6b), the energy shifts can be transferred to the strain (stress) scale. Figure 10 shows the thickness dependence of the strain and stress. The open and solid circles in Fig. 10 are calculated from the data in groups A and B in Fig. 9, respectively. The obtained strain profile reflects the presence of the systematic change in the strain of two different strain regions in one sample. The open circles show that compressive strain exists in one region at the initial stage of the growth and is gradually relaxed. Then this region transfers to tensile strain around thicknesses greater than 2 μm. It is noted that for thicknesses around 2 μm, the compressive stress balances with thermally induced tension. In the other region (solid circles), tensile strain exists. This region has a band-edge energy of about E_g^0 at about 0.5 μm, and the tensile strain becomes large with increasing thickness. However, this

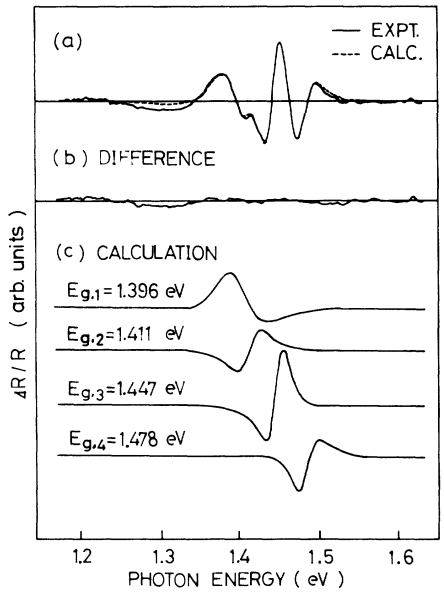

FIG. 8. Low-field PR spectrum [solid line in (a)] of GaAs (undoped) at 0.84 μm and theoretically calculated PR spectrum [dotted line in (a)]. The difference between them is plotted in (b). Calculated spectrum consists of four interband-edge spectra shown in (c).

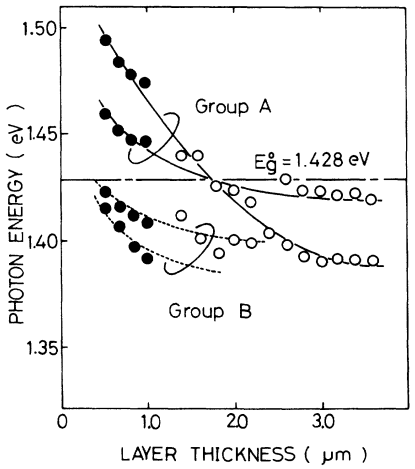

FIG. 9. Thickness dependence of $E_{g,j}$: the open and solid circles denote the data of Figs. 4 and 6, respectively. Dash-dotted line shows the position of the band edge of GaAs with no strain (E_g^0 = 1.428 eV).

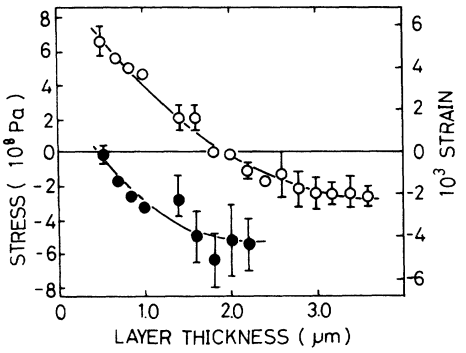

FIG. 10. Stress and strain calculated from Fig. 9. The open and solid circles are calculated from the data in groups *A* and *B* in Fig. 9, respectively.

region disappears around thicknesses greater than 2 μm. These large thickness dependences of strain are quite different from the theoretical estimation by the thermal-expansion mismatch (Fig. 3), in which the strain slightly changes in the thickness range 0.5–3.6 μm. Our experimental results indicate that the compressive stress due to the lattice mismatch between GaAs and Si should be taken into account together with thermal effects. Ogasawara *et al.*[8] pointed out that there is a relaxation mechanism produced by a compressive stress component in the thermally induced strain system, when GaAs is grown at relatively low temperature (< 600 °C). In particular, it has been noted that the materials grown below 420 °C show only compressive strain.[8] In this experiment, GaAs was grown at 570 °C, which is relatively low in comparison with the substrate temperature reported previously.[6,7,10,11] The observed transition from compression to tension demonstrates the presence of the relaxation process produced by a tensile component in GaAs grown at low temperature on a Si substrate.

V. CONCLUSIONS

Single-crystalline GaAs was grown directly on a Si substrate at a relatively low growth temperature (570 °C). The residual strain in the epitaxial film was investigated by PR measurements. PR signals measured at room temperature were very clear, and this led to the reliable assignment of the fundamental band edge.

The observed PR spectra indicate that the hydrostatic component of the residual strain in the heteroepitaxial film induces a shift of center of gravity of the $P_{2/3}$ multiplet and that the biaxial component splits this multiplet. The compressive strain caused by the lattice mismatch is not completely compensated by the formation of misfit dislocations during the growth, but the compressive component is gradually relaxed by the tensile component originating from the thermal-expansion mismatch. For thicknesses greater than 2 μm, only tensile strain was observed, while in the thickness range from 0.5 to 2.0 μm, the observed PR spectrum reflected the presence of two different strain regions in one sample of GaAs on a Si substrate. Furthermore, for thicknesses less than 0.5 μm, the crystal quality was degraded by defects associated with the misfit compensation during the initial stage of growth.

A clear difference in the PR signal has been found with the impurity concentrations in the GaAs layer. The spectral line shapes of highly doped and undoped samples are well explained by FK oscillations and the derivativelike feature in the low-field regime, respectively. In the low-field regime, the PR spectrum was expressed by a third-derivative line shape of the dielectric function, and the pumping-light-power dependence of the amplitude of modulated reflectance was well explained by the photovoltaic effect. In the intermediate-field regime, FK oscillations were observed. The period and envelope function of these FK oscillations are related to the built-in and modulating surface electric field. According to a generalized FK theory in which a large built-in electric field is taken into account, the built-in electric field and built-in potential at the surface of GaAs film on a Si substrate were determined. The obtained value was somewhat smaller than that expected under Fermi-level pinning.

ACKNOWLEDGMENTS

The authors would like to thank Professor M. Okuyama of Osaka University for his useful discussions and Professor K. Kubota of Kwansei Gakuin University for his constant encouragement. The authors would also like to thank Dr. S. Yasuda of Kao Corporation for supplying vitreous carbon crucibles for KOH etching in the EPD measurement.

[1]T. H. Windhorm, G. H. Metze, B. Y. Tsaur, and J. C. C. Fan, Appl. Phys. Lett. **45**, 309 (1984).

[2]R. W. Kaliski, N. Holonyak, Jr., K. C. Hsieh, D. W. Nam, J. W. Lee, H. Shichijo, R. D. Bumham, J. E. Epler, and H. F. Chung, Appl. Phys. Lett. **50**, 836 (1987).

[3]H. K. Choi, B. Y. Tsaur, G. M. Metze, G. W. Turner, and J. C. C. Fan, IEEE Electron Device Lett. **EDL-5**, 207 (1984).

[4]H. Morkoç, C. K. Peng, T. Henderson, W. Kopp, R. Fischer, L. P. Erickson, M. D. Longerbone, and R. C. Youngman, IEEE Electron Device Lett. **EDL-6**, 381 (1985).

[5]Y. Itoh, T. Nishioka, A. Yamamoto, and M. Yamaguchi, Appl. Phys. Lett. **52**, 1617 (1988).

[6]B. A. Wilson, C. E. Bonner, R. C. Miller, S. K. Sputz, T. D. Harris, M. G. Lamont, R. D. Dupuis, S. M. Vernon, V. E. Haven, R. M. Lum, and J. K. Klingert, J. Electron. Mater. **17**, 115 (1988).

[7]N. Lucas, H. Zabel, H. Morkoç, and H. Unlu, Appl. Phys. Lett. **52**, 2117 (1988).

[8]K. Ogasawara and K. Kondo, Jpn. J. Appl. Phys. Pt. 2 **27**, L1736 (1988).

[9]T. D. Harris, M. G. Lamont, R. Sauer, R. M. Lum, and J. K. Klingert, J. Appl. Phys. **64**, 5110 (1988).

[10]R. M. Lum, J. K. Klingert, R. B. Bylsma, A. M. Glass, A. T. Macrander, T. D. Harris, and M. G. Lamont, J. Appl. Phys. **64**, 6727 (1988).

[11]M. Sugo, N. Uchida, A. Yamamoto, T. Nishioka, and M.

Yamaguchi, J. Appl. Phys. **65**, 591 (1989).
[12]J. L. Shay, Phys. Rev. B **2**, 803 (1970).
[13]H. Shen, X. C. Shen, F. H. Pollak, and R. N. Sacks, Phys. Rev. B **36**, 3487 (1987).
[14]R. N. Battacharya, H. Shen, P. Parayanthal, F. H. Pollak, T. Coutts, and H. Aharoni, Phys. Rev. B **37**, 4044 (1988).
[15]H. Shen, Z. Hang, S. H. Pan, F. H. Pollak, and J. M. Woodall, Appl. Phys. Lett. **52**, 2058 (1988).
[16]H. Shen, S. H. Pan, Z. Hang, J. Leng, F. H. Pollak, J. M. Woodall, and R. N. Sacks, Appl. Phys. Lett. **53**, 1080 (1988).
[17]O. J. Glembocki, B. V. Shanabrook, N. Botta, W. T. Beard, and J. Comas, Appl. Phys. Lett. **46**, 970 (1985).
[18]H. Shen, P. Paryanthal, F. H. Pollak, M. Tomkiewicz, J. J. Drummond, and J. N. Schulman, Appl. Phys. Lett. **48**, 653 (1986).
[19]U. K. Reddy, G. Ju, T. Henderson, H. Morkoç, and J. N. Schulman, J. Appl. Phys. **62**, 145 (1987).
[20]W. M. Theis, G. D. Sanders, C. E. Leak, D. C. Reynolds, Y. C. Chang, K. Alavi, C. Colvard, and I. Shidlovsky, Phys. Rev. B **39**, 1442 (1989).
[21]F. H. Pollak, M. Cardona, and K. L. Shaklee, Phys. Rev. Lett. **16**, 942 (1966).
[22]F. H. Pollak and M. Cardona, Phys. Rev. **172**, 816 (1968).
[23]M. Chandrasekhar and F. H. Pollak, Phys. Rev. B **15**, 2127 (1977).
[24]J. H. Neave, B. A. Joyce, P. J. Dobson, and N. Norton, Appl. Phys. A **31**, 1 (1983).
[25]A. Ishizaka, K. Nakagawa, and Y. Shiraki (unpublished).
[26]Z. Feng and H. Liu, J. Appl. Phys. **54**, 83 (1983).
[27]See, for example, D. E. Aspnes, in *Handbook of Semiconductors,* edited by T. S. Moss (North-Holland, Amsterdam, 1980), Vol. 2, p. 109, and references therein.
[28]D. E. Aspnes, Surf. Sci. **37**, 418 (1973).
[29]D. E. Aspnes, Phys. Rev. **153**, 972 (1967).
[30]R. P. Silberstein and F. H. Pollak, Solid State Commun. **33**, 1131 (1980).
[31]W. E. Spicer, I. Lindu, P. Skeath, and C. Y. Su, J. Vac. Sci. Technol. **17**, 1019 (1980).
[32]H. Takakura, M. Matsunaga, T. Kanata, and Y. Hamakawa (unpublished).